Journal of the Mechanics and Physics of Solids xxx (xxxx) xxx

Contents lists available at ScienceDirect

Journal of the Mechanics and Physics of Solids

journal homepage: www.elsevier.com/locate/jmps

Nonlinear transition waves in free-standing bistable chains

Bolei Deng[a], Pai Wang[a,b], Vincent Tournat[c], Katia Bertoldi[a,d,*]

[a] Harvard John A. Paulson School of Engineering and Applied Sciences, Harvard University, Cambridge, MA 02138, USA
[b] Department of Mechanical Engineering, University of Utah, Salt Lake City, Utah 84112, USA
[c] LAUM UMR 6613, CNRS, Le Mans Université, Le Mans 72085, France
[d] Kavli Institute, Harvard University, Cambridge, MA 02138, USA

ARTICLE INFO

Article history:
Received 16 April 2019
Revised 2 July 2019
Accepted 5 July 2019
Available online xxx

Keywords:
Transition waves
Bistability
Non-linear dynamics

ABSTRACT

We propose an analytical framework to study the propagation of transition waves in one-dimensional free-standing lattices comprising concentrated masses and bistable springs. Starting from the discrete model, we derive the partial differential equation that describes the non-linear dynamic response of the system and obtain its exact closed-form solution. Such solution enables us to uncover the effect of the system's parameters on the characteristics of the supported transition waves as well as to characterize the rarefaction front that precedes the pulse. As such, this work provides new opportunities to elucidate how transition waves propagate in systems in which the phase transition results in macroscopic volumetric changes.

1. Introduction

From ferroelectric materials (Giri et al., 2012; Wojnar et al., 2014) and mechanical metamaterials (Frazier and Kochmann, 2017; Nadkarni et al., 2016a; Raney et al., 2016) to shape memory alloys (Dye, 2015) and multiferroics (Fiebig et al., 2016), transition waves (also referred to as elastic topological solitons) play a central role in a multitude of materials and structures. Although these systems are very different in both structure and composition, they are all made of elements that possess two or more stable equilibrium states and can snap from one to another. By applying a stimulus large enough to overcome the initial energy barrier, a transition wave is initiated that sequentially switches all the units from an higher-energy stable configuration into a lower-energy one. The energy released during such switching compensate for the energy dissipated during the process and, ultimately, allows propagation over long distances (Nadkarni et al., 2016a; Raney et al., 2016).

To get more insight into the propagation of such non-linear waves, a number of discrete models comprising rigid masses and bistable springs have been proposed and investigated (Braun and Kivshar, 1998; Comte et al., 1999; Nadkarni et al., 2016b; 2014; Remoissenet and Peyrard, 1984; Slepyan, 2000; 2001; Slepyan et al., 2005; Truskinovsky and Vainchtein, 2005). For lattices with bistable springs that connect the rigid masses to the ground analytical closed-form solutions have been obtained (Braun and Kivshar, 1998; Comte et al., 1999; Nadkarni et al., 2016b; 2014; Remoissenet and Peyrard, 1984), which explicitly define the effect of system's parameters on the speed and width of the supported transition waves. However, such models cannot be used to capture important physical phenomena such as martensite phase transition and fracture. To overcome this issue, the behavior of free-standing chains with bistable springs has been investigated (Slepyan et al., 2005; Truskinovsky and Vainchtein, 2005), but only solutions via series expansion have been found, limit-

* Corresponding author at: Harvard John A. Paulson School of Engineering and Applied Sciences, Harvard University, Cambridge, MA 02138, USA.
E-mail address: bertoldi@seas.harvard.edu (K. Bertoldi).

https://doi.org/10.1016/j.jmps.2019.07.004
0022-5096/

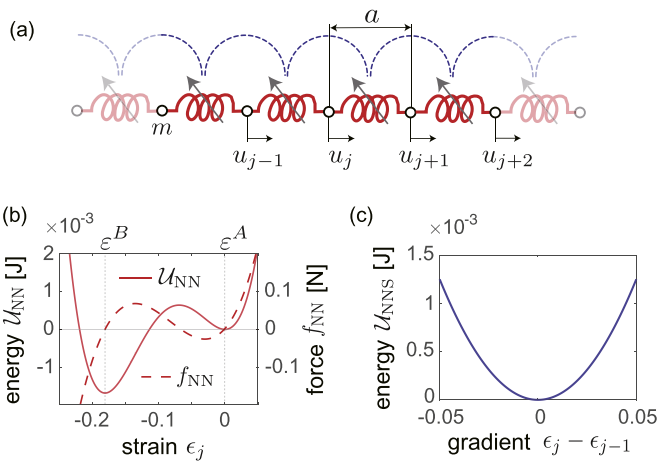

Fig. 1. (a) Our system consists of a 1D array of masses m, connected by bistable springs. Moreover, we also consider nearest neighboring spring interactions (indicated by the dashed blue lines). (b) Evolution of the strain energy (continuous line) and force (dashed line) as a function of the strain ε_j for the bistable springs. The two stable configurations of the bistable elements correspond to the strain ε^A and ε^B. (c) Evolution of $\mathcal{U}_{NNS}$ as a function of the strain gradient $\varepsilon_j - \varepsilon_{j-1}$. (For interpretation of the references to colour in this figure legend, the reader is referred to the web version of this article.)

ing the physical understanding of the relation between the structural parameters and the characteristics of the supported transition waves.

In this paper, we study the propagation of non-linear waves in a free-standing lattice comprising a one dimensional (1D) array of rigid masses connected to their nearest neighbors by bistable springs. First, we derive the discrete governing equations and solve them numerically to find that (*i*) the considered chain supports the propagation of transition waves that sequentially brings all springs from their higher energy stable configuration to the lower-energy one; and that (*ii*) such waves are preceded by a rarefaction front that stretches the springs. Second, to gain deeper insight into the dynamics of the system, we derive the continuum governing equation. Remarkably, we find that such continuum equation admits closed-form solutions, which enable us to accurately predict the strain and velocity of the units before and after the propagation of the transition waves as well as the characteristics of the wavefront as a function of system's parameter.

This paper is organized as follows. First, in Section 2 we present our system comprising a 1D array of masses connected by bistable springs. Then, in Section 3 we describe the discrete model established to characterize the propagation of transition waves though the chain. Finally, in Section 4 we derive a continuum model, obtain its analytical solution and use it to explore the effect of system's parameters.

2. Our system

In this study we consider a 1D array of identical masses m separated by a distance a from each other and constrained to move only in longitudinal direction (see Fig. 1(a)). The j-th mass is connected to $j-1$th mass via a nearest neighbor (NN) non-linear spring with potential

$$\mathcal{U}_{\rm NN}(\varepsilon_j) = \frac{1}{2}B_1\varepsilon_j^2 + \frac{1}{3}B_2\varepsilon_j^3 + \frac{1}{4}B_3\varepsilon_j^4, \tag{1}$$

where B_1, B_2 and $B_3 > 0$ are constants and ε_j denotes the strain of the jth spring, which is defined as

$$\varepsilon_j = \frac{u_j - u_{j-1}}{a}, \tag{2}$$

u_j being the displacement of the jth mass in longitudinal direction. If $B_2^2 > 4B_1B_3$, the energy landscape defined by Eq. (1) is characterized by two local minima located at (see Fig. 1(b))

$$\varepsilon^A = 0, \quad \varepsilon^B = \frac{-B_2 - \sqrt{B_2^2 - 4B_1B_3}}{2B_3}, \tag{3}$$

so that the jth spring has two stable equilibrium configurations. For the energy function considered in this study the stable configuration at ε^B is always characterized by an energy state lower than that at ε^A, so that

$$\Delta\mathcal{U}_{\rm NN} = \mathcal{U}_{\rm NN}(\varepsilon^B) - \mathcal{U}_{\rm NN}(\varepsilon^A) < 0. \tag{4}$$

Finally, we note that the force in the jth NN spring

$$f_{\rm NN}(\varepsilon_j) = \frac{1}{a}\frac{{\rm d}\mathcal{U}_{\rm NN}(\varepsilon_j)}{{\rm d}\varepsilon_j} = \frac{1}{a}\left(B_1\varepsilon_j + B_2\varepsilon_j^2 + B_3\varepsilon_j^3\right), \tag{5}$$

Please cite this article as: B. Deng, P. Wang and V. Tournat et al., Nonlinear transition waves in free-standing bistable chains, Journal of the Mechanics and Physics of Solids, https://doi.org/10.1016/j.jmps.2019.07.004

is highly nonlinear and both negative and positive for applied compressive strains (see Fig. 1(b)).

Besides the non-linear springs, we also consider nearest neighboring spring (NNS) interactions (see dashed connections in Fig. 1(a)) and capture their response via the quadratic potential (see Fig. 1(c))

$$\mathcal{U}_{\mathrm{NNS}}\left(\varepsilon_j-\varepsilon_{j-1}\right)=\frac{G}{2}\left(\varepsilon_j-\varepsilon_{j-1}\right)^2, \tag{6}$$

$G>0$ being a constant. Note that such NNS interactions have a similar effect as next nearest neighbor interactions and have been shown to be important to accurately capture the response of 2D/3D systems via a simple 1D model (Audoly and Hutchinson, 2016; Rafsanjani et al., 2019), to model the formation and propagation of shear bands in plastic flow (Aifantis, 1992) as well as to regularize the problem and enable analytical solutions (Truskinovsky and Vainchtein, 2005). Finally, we want to point out that the interactions defined by Eq. (6) can significantly alter the energy landscape of the system as they tend to reduce the difference in strain between neighbouring NN springs. Moreover, if G is large enough to overcome the initial energy barrier, these interactions can destabilize a chain in which some of the NN springs are in the undeformed stable configuration (i.e. springs for which $\varepsilon_j=\varepsilon^A$) and other in the deformed one (i.e. springs for which $\varepsilon_j=\varepsilon^B$), triggering the propagation of a large amplitude wave that switches all springs in the higher-energy stable state to the lower-energy one. In the remaining of this paper, we use a combination of numerical analysis and theory to study in detail the propagation of such large amplitude non-linear waves in our system.

3. Discrete model

We begin by deriving the governing equations of the chain and solving them numerically to characterize the transition wave propagation. To this end, we first note that the Lagrangian of the system described in Section 2 is given by

$$L=\sum_{i=1}^{n}\frac{1}{2}m\left(\frac{\mathrm{d}u_j}{\mathrm{d}t}\right)^2-\mathcal{U}_{\mathrm{NN}}\left(\varepsilon_j\right)-\mathcal{U}_{\mathrm{NNS}}\left(\varepsilon_j-\varepsilon_{j-1}\right), \tag{7}$$

from which the equilibrium equation can be derived using Lagrange's equations as

$$m\frac{\mathrm{d}^2u_j}{\mathrm{d}t^2}=f_{\mathrm{NN}}\left(\varepsilon_{j+1}\right)-f_{\mathrm{NN}}\left(\varepsilon_j\right)-f_{\mathrm{NNS}}\left(\varepsilon_{j+2}-\varepsilon_{j+1}\right)+2f_{\mathrm{NNS}}\left(\varepsilon_{j+1}-\varepsilon_j\right)-f_{\mathrm{NNS}}\left(\varepsilon_j-\varepsilon_{j-1}\right), \tag{8}$$

where ε_j is defined in Eq. (2) and

$$f_{\mathrm{NNS}}(\varepsilon_j-\varepsilon_{j-1})=\frac{1}{a}\frac{\mathrm{d}\mathcal{U}_{\mathrm{NNS}}(\varepsilon_j-\varepsilon_{j-1})}{\mathrm{d}(\varepsilon_j-\varepsilon_{j-1})}=\frac{G}{a}(\varepsilon_j-\varepsilon_{j-1}). \tag{9}$$

Eq. (8) represents the discrete governing equation of the system, which we numerically solve using the 4th order Runge-Kutta method (via the Matlab function ode45 - see Supporting Information for the Matlab code).

In Fig. 2 we present numerical results for a chain with $n=2500$ masses with $m=10$ g, $a=1$ cm, $B_1=1$ J, $B_2=20$ J, $B_3=80$ J and $G=1$ J, so that $\varepsilon^A=0$, $\varepsilon^B=-0.181$, $\Delta\mathcal{U}_{\mathrm{NN}}=-1.7\times10^{-3}$J (see Fig. 1(b)) and linear vibrations in the long wavelength limit propagate with velocity $c_0=\sqrt{B_1/m}=10$ m/s. In our simulations all masses are initially displaced according to (see Fig. 2(a))

$$u_j=\begin{cases}a\,\varepsilon^B(j-10), & \text{if } j\le 10.\\ 0, & \text{otherwise,}\end{cases} \tag{10}$$

so that

$$\varepsilon_j=\begin{cases}\varepsilon^B, & \text{if } j\le 10,\\ \varepsilon^A, & \text{otherwise.}\end{cases} \tag{11}$$

Therefore, all NN springs are initially in their higher-energy stable configuration at ε^A (which we also refer to as phase A), except for the first 10 that are set to their deformed lower-energy configuration at ε^B (which we also refer to as phase B). Then, at time $t=0$ we release all masses and monitor their displacement. We find that the initial configuration is unstable and the NN springs in the higher-energy minimum (phase A) sequentially transition to the lower-energy deformed stable state (phase B), producing a nonlinear transition wave that propagates toward the right with constant velocity $c=3.01$ m/s (see Fig. 2(b)). Note that this wave is qualitatively different from those recently observed in 1D mechanical metamaterials comprising an array of coupled bistable units (Nadkarni et al., 2014; Raney et al., 2016), since in those systems all elements have vanishing velocity after transition (since their end points of are rigidly attached to the ground). By contrast, in our system the jth bistable spring keeps moving forward after transition until the wave reaches the end of the chain (see Fig. 2(c)). As such, the propagation of the transition wave in our system requires potential energy to transfer into kinetic energy and, therefore, is only possible if each spring releases energy when, stimulated by the wavefront, it transitions from one stable state to the other one.

The results of Fig. 2(b) also show that the NN springs immediately to the right of phase B are not in phase A (i.e., in their undeformed configuration), but stretched to an average strain of $\approx$0.140. This indicates there is a rarefaction front (which

Please cite this article as: B. Deng, P. Wang and V. Tournat et al., Nonlinear transition waves in free-standing bistable chains, Journal of the Mechanics and Physics of Solids, https://doi.org/10.1016/j.jmps.2019.07.004

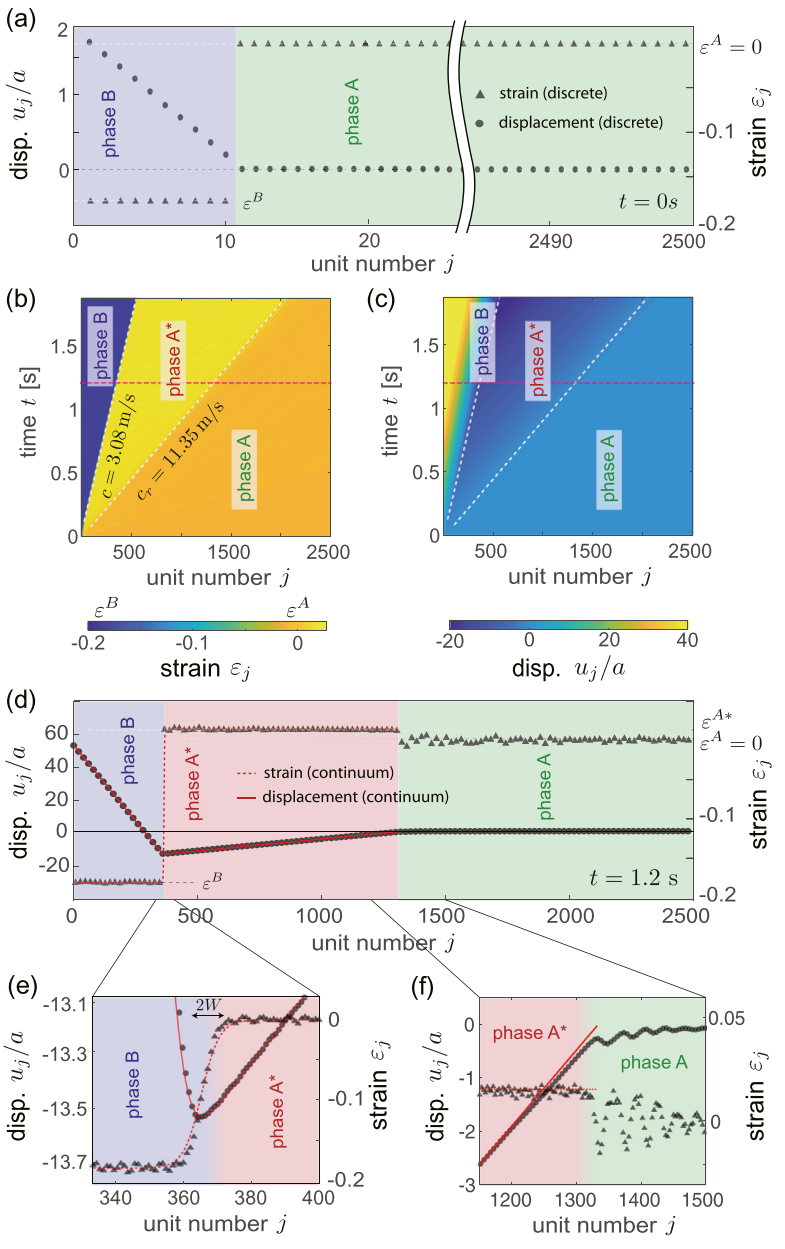

Fig. 2. (a) In our numerical simulations all NN springs are initially in the undeformed stable configuration, except for the first 10 that are compressed to their deformed stable configuration. (b) Strain of the NN springs and (c) displacement of the masses during the propagation of the pulse as predicted by our discrete model. (d) Evolution of u_j (left axis) and ε_j (right axis) along the chain at $t = 1.2$ s. (e) Zoom-in of the transition zone between NN springs with strain ε^B and ε^{A*}. (f) Zoom-in of the transition zone between NN springs with strain ε^{A*} and ε^A. In (d)-(f) markers correspond to numerical results and continuous lines to the analytical predictions. Note that the oscillatory tail ahead of the rarefaction front is due to the imposed initial conditions..

we refer to as phase A^*) that propagates ahead of the transition wave. This front is also clearly visible in Fig. 2(d), where we report the evolution of u_j and ε_j along the chain at time $t = 1.2$ s and observe three well-separated phases (phase A, phase B and phase A^*). Finally, our results also indicate that this rarefaction front propagates without apparent distortion with a constant supersonic velocity $c_r = 11.35$ m/s.

To further investigate the response of our system, in Fig. 3 we report the strain, ε_j, and velocity, $v_j^{\mathrm{NN}} = (v_j + v_{j-1})/2$ (v_j denoting the velocity of the j-th mass), of the first 500 NN springs during the propagation of the transition wave. In this phase diagram three well-defined clusters clearly emerge, characterized by different strain and velocity. Initially all units are undeformed and at rest (phase A with $\varepsilon_j = 0$ and $v_j = 0$). Then, they stretch to $\varepsilon_j \approx 0.014$ and acquire a negative velocity of $\approx$-0.16 m/s (phase A^*). Finally, they transition to the lower-energy stable configuration at $\varepsilon^B = -0.181$ (phase B) and, in stark

Please cite this article as: B. Deng, P. Wang and V. Tournat et al., Nonlinear transition waves in free-standing bistable chains, Journal of the Mechanics and Physics of Solids, https://doi.org/10.1016/j.jmps.2019.07.004

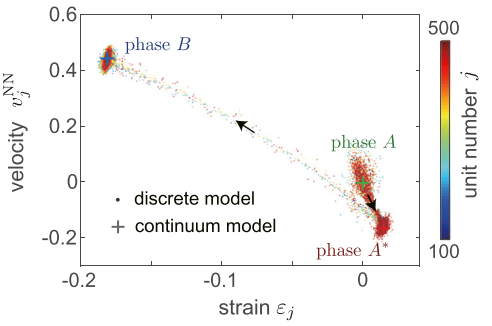

Fig. 3. Evolution of the strain ε_j and velocity, $v_j^{NN} = (v_j + v_{j-1})/2$ of first 500 NN springs during the propagation of the transition wave. Circular markers correspond to numerical results and crosses to the theoretical predictions (via Eq. (40)).

contrast to the previously reported bistable metamaterial chains (Nadkarni et al., 2014; Raney et al., 2016), keep translating at constant velocity ≈ 0.44 m/s.

4. Continuum model

Next, to better understand the propagation of transition waves in our system, we derive an analytical solution. To this end, we first calculate the difference of Eq. (8) at site j and site $j-1$, which gives

$$a\,m\frac{\mathrm{d}^2\varepsilon_j}{\mathrm{d}t^2} = f_{\mathrm{NN}}\left(\varepsilon_{j+1}\right) - 2f_{\mathrm{NN}}\left(\varepsilon_j\right) + f_{\mathrm{NN}}\left(\varepsilon_{j-1}\right) - \frac{G}{a}\left(\varepsilon_{j+2} - 4\varepsilon_{j+1} + 6\varepsilon_j - 4\varepsilon_{j-1} + \varepsilon_{j-2}\right), \tag{12}$$

where Eq. (9) is applied. Next, two continuous functions $\varepsilon(x)$ and $u(x)$ are introduced to interpolate the discrete variables ε_j and u_j as

$$\varepsilon\left(x = x_j,\, t\right) = \varepsilon_j(t), \quad \text{and} \quad u\left(x = x_j + \frac{a}{2}, t\right) = u_j(t), \tag{13}$$

where $x_j = j\,a$ denotes the position of the jth mass when all springs are undeformed. Moreover, we assume that the width of the propagating front, w, is much larger than a and use Taylor expansion to express any function $f(x,\,t)$ at x_{j+p} as

$$f\left(x_{j+p},\,t\right) = \left[f + a\,p\,\partial_x f + \frac{(a\,p)^2}{2}\partial_{xx} f + \frac{(a\,p)^3}{6}\partial_{xxx} f + \frac{(a\,p)^4}{24}\partial_{xxxx} f\right]_{x_j,\,t} + \mathrm{o}\left(\frac{a^4}{w^4}\right), \tag{14}$$

where p is a real number and $\partial_\alpha f = \partial f/\partial\alpha$. By introducing Eqs. (13) and (14) into Eq. (2) we find

$$\varepsilon\left(x = x_j,\, t\right) = \partial_x u(x = x_j,\, t) + \mathrm{o}\left(\frac{a^2}{w^2}\right), \tag{15}$$

which provides a relation between the continuous functions u and ε. Moreover, substitution of Eqs. (13) and (14) into Eqs. (12) yields the continuum governing equation,

$$m\,\partial_{tt}\varepsilon = a\,\partial_{xx}\,f_{\mathrm{NN}}(\varepsilon) + a^2\partial_{xxxx}\left[\frac{a}{12}f_{\mathrm{NN}}(\varepsilon) - G\,\varepsilon\right] + \mathrm{o}\left(\frac{a^4}{w^4}\right), \tag{16}$$

Since for our system (for which $G = 1$ J) $G\,\varepsilon \gg a f_{\mathrm{NN}}/12$ (see Fig. 1(b)), in an attempt to obtain analytical solution, we omit the term associated with the local energy barrier and further simplify Eq. (16) as

$$m\,\partial_{tt}\varepsilon = a\,\partial_{xx}\,f_{\mathrm{NN}}(\varepsilon) - a^2 G\,\partial_{xxxx}\,\varepsilon. \tag{17}$$

Eq. (17) can be rewritten in terms of the traveling wave coordinate $\zeta = x - ct$ (c being the pulse velocity) as

$$m\,c^2\mathrm{d}_{\zeta\zeta}\varepsilon = a\,\mathrm{d}_{\zeta\zeta} f_{\mathrm{NN}}(\varepsilon) - a^2 G\,\mathrm{d}_{\zeta\zeta\zeta\zeta}\varepsilon, \tag{18}$$

where $\mathrm{d}_\zeta f = df/d\zeta$. Next, we integrate Eq. (18) twice with respect to ζ to obtain

$$a^2 G\,\mathrm{d}_{\zeta\zeta}\varepsilon = a\,f_{\mathrm{NN}}(\varepsilon) - mc^2\varepsilon + C_1\zeta + C_2, \tag{19}$$

where C_1 and C_2 are integration constants. Since in our chain the nonlinear wave that transitions the bistable springs from the higher-energy stable state at ε^A to the lower-energy one at ε^B propagates from left to right, we impose

$$\varepsilon(\zeta \to -\infty) = \varepsilon^B, \tag{20}$$

and find

$$C_1 = 0 \quad \text{and} \quad C_2 = m\,c^2\varepsilon^B, \tag{21}$$

Please cite this article as: B. Deng, P. Wang and V. Tournat et al., Nonlinear transition waves in free-standing bistable chains, Journal of the Mechanics and Physics of Solids, https://doi.org/10.1016/j.jmps.2019.07.004

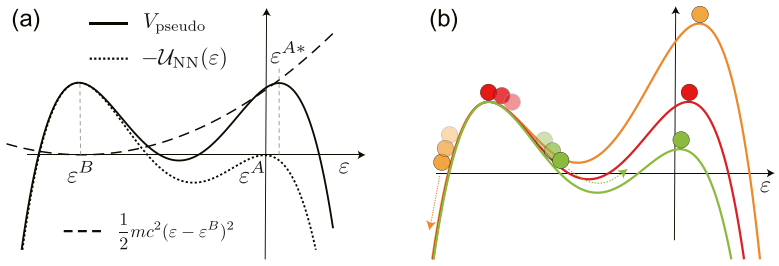

Fig. 4. (a) Evolution of $\mathcal{U}_{\text{NN}}$, $1/2mc^2(\varepsilon-\varepsilon^B)^2$ and V_{pseudo} as a function of ε. (b) Depending on c, we may have either (*i*) $V_{\text{pseudo}}(\varepsilon^{A*}) < V_{\text{pseudo}}(\varepsilon^B)$ (green line); (*ii*) $V_{\text{pseudo}}(\varepsilon^{A*}) > V_{\text{pseudo}}(\varepsilon^B)$ (orange line) or (*iii*) $V_{\text{pseudo}}(\varepsilon^{A*}) = V_{\text{pseudo}}(\varepsilon^B)$ (red line). (For interpretation of the references to colour in this figure legend, the reader is referred to the web version of this article.)

so that Eq. (19) can be rewritten as

$$a^2 G\, \mathrm{d}_{\zeta\zeta}\varepsilon = a\, f_{\text{NN}}(\varepsilon) - m\, c^2(\varepsilon-\varepsilon^B). \tag{22}$$

Finally, to obtain analytical solution, we multiply Eq. (22) by $\mathrm{d}_\zeta\varepsilon$ and integrate it with respect to ζ to get

$$\frac{1}{2}(a^2G)\left(\varepsilon_\zeta\right)^2 - \mathcal{U}_{\text{NN}}(\varepsilon) + \frac{1}{2}mc^2(\varepsilon-\varepsilon^B)^2 = 0, \tag{23}$$

where we have set the integration constant equal to zero. Interestingly, Eq. (23) can be viewed as the sum of the kinetic energy (with respect to the pseudo-time ζ) and the potential energy of a fictitious particle of mass a^2G (Dauxois and Peyrard, 2006). Thus, the solution $\varepsilon(\zeta)$ of Eq. (23) describes the motion of such particle in the potential

$$V_{\text{pseudo}}(\varepsilon) = -\mathcal{U}_{\text{NN}}(\varepsilon) + \frac{1}{2}mc^2(\varepsilon-\varepsilon^B)^2, \tag{24}$$

which incorporates the contribution of both the bi-stable springs and the speed of the propagating transition waves and is typically characterized by two local maxima, one located at ε^B and one at a strain ε^{A*} slightly larger than ε^A (see Fig. 4(a)- we will show later that ε^{A*} corresponds to the strain induced by the rarefaction precursor). While the maximum at ε^B only depends on the properties of the springs, the one at ε^{A*} is also affected by the speed of the propagating wave. Depending on c, we may have either (*i*) $V_{\text{pseudo}}(\varepsilon^{A*}) < V_{\text{pseudo}}(\varepsilon^B)$; (*ii*) $V_{\text{pseudo}}(\varepsilon^{A*}) > V_{\text{pseudo}}(\varepsilon^B)$ or (*iii*) $V_{\text{pseudo}}(\varepsilon^{A*}) = V_{\text{pseudo}}(\varepsilon^B)$ (see Fig. 4(b)). If $V_{\text{pseudo}}(\varepsilon^{A*}) < V_{\text{pseudo}}(\varepsilon^B)$, a ficticious particle leaving ε^{A*} at rest cannot reach ε^B and returns to $\varepsilon = \varepsilon^{A*}$ - a scenario that corresponds to a solitary pulse that propagates in the chain without transitioning the bistable springs from one stable state to the other (Katz and Givli, 2018). Differently, if $V_{\text{pseudo}}(\varepsilon^{A*}) > V_{\text{pseudo}}(\varepsilon^B)$, the ficticious particle reaches ε^B with non-zero velocity $d\varepsilon/d\zeta$, keeps sliding and never goes back to ε^{A*} - a situation that corresponds to a non-physical diverging solution of equation Eq. (22). Finally, if $V_{\text{pseudo}}(\varepsilon^{A*}) = V_{\text{pseudo}}(\varepsilon^B)$, a fictitious particle leaving the peak at ε^{A*} at rest can reach the one at ε^B with a vanishing velocity and this corresponds to a transition wave that brings each unit from one stable configuration to the other one. As such, the velocity of the transition wave that switches the NN springs from $\varepsilon^{A*} > 0$ to ε^B can be found by imposing

$$V_{\text{pseudo}}(\varepsilon^{A*}) = V_{\text{pseudo}}(\varepsilon^B), \tag{25}$$

with

$$\mathrm{d}_\varepsilon V_{\text{pseudo}}(\varepsilon^{A*}) = 0 \quad \text{and} \quad \mathrm{d}_{\varepsilon\varepsilon} V_{\text{pseudo}}(\varepsilon^{A*}) < 0. \tag{26}$$

By substituting Eqs. (1), (3) and (24) into Eqs. (25) and (26) we find that these are identically satisfied only if

$$c = \sqrt{\frac{B_2\,\varepsilon^{A*}}{3m}} \quad \text{and} \quad \varepsilon^{A*} = -\varepsilon^B - \frac{2B_2}{3B_3}, \tag{27}$$

which give the explicit expressions of propagating velocity c and rarefaction strain ε^{A*} as functions of structural parameters. Under these conditions Eq. (27) can be rewritten as

$$\mathrm{d}_{\zeta\zeta}\varepsilon = \frac{B_3}{a^2G}\left(\varepsilon-\varepsilon^{A*}\right)\left(\varepsilon-\varepsilon^B\right)\left(\varepsilon - \frac{\varepsilon^{A*}+\varepsilon^B}{2}\right). \tag{28}$$

Eq. (28) has the form of a nonlinear Klein-Gordon equation and admits analytical solutions of the form (Polyanin and Zaitsev, 2011; Rafsanjani et al., 2019; Wazwaz, 2007)

$$\varepsilon = \frac{\varepsilon^{A*}+\varepsilon^B}{2} + \frac{\varepsilon^{A*}-\varepsilon^B}{2}\tanh\left(\frac{x-c(t-t_0)}{W}\right), \tag{29}$$

Please cite this article as: B. Deng, P. Wang and V. Tournat et al., Nonlinear transition waves in free-standing bistable chains, Journal of the Mechanics and Physics of Solids, https://doi.org/10.1016/j.jmps.2019.07.004

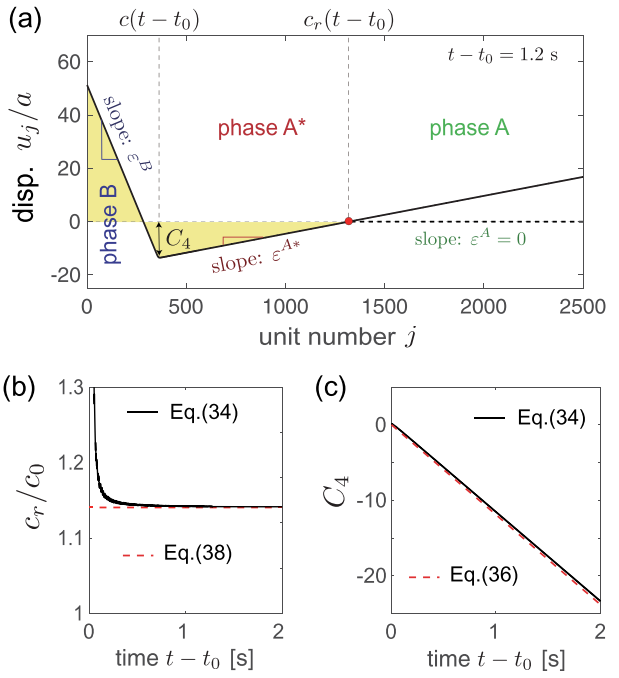

Fig. 5. (a) Evolution of u along the chain at $t-t_0 = 1.2$ s. In a finite size chain $u^{\text{finite}}(x,t) = 0$ for $x > c_r(t-t_0)$. (b)-(c) Evolution of (b) c_r/c_0 and (c) C_4 as a function of $t-t_0$. Continuous lines correspond to the solution found by numerically solving Eq. (34), while dashed lines correspond to the analytical solution provided by Eqs. (38) and (36).

where

$$W = \frac{4a}{\varepsilon^{A*}-\varepsilon^B}\sqrt{\frac{G}{2B_3}} = \frac{6a\sqrt{2B_3G}}{B_2+3\sqrt{B_2^2-4B_1B_3}}, \tag{30}$$

denotes the width of the transition wave and t_0 is the time at which the pulse starts.

Finally, the displacement induced by the transition wave during its propagation can be obtained as

$$u(x,t) = \int \varepsilon\, \mathrm{d}x = \frac{W(\varepsilon^{A*}-\varepsilon^B)}{2}\ \ln\left[\cosh\left(\frac{x-c(t-t_0)}{W}\right)\right] + \frac{\varepsilon^{A*}+\varepsilon^B}{2}\,[x-c(t-t_0)] + C_4(t), \tag{31}$$

where $C_4(t)$ is the integration constant which corresponds to a rigid body motion of the entire chain (since $u|_{x=c(t-t_0)} = C_4(t)$). In Fig. 5(a) we report the displacement along the chain described by Eq. (31) at $t-t_0 = 1.2$ s. We find that u has a negative slope equal to ε^B for $x \lesssim c(t-t_0)$, it reaches $C_4(t)$ at $x = c(t-t_0)$ and then has a positive slope equal to ε^{A*} for $x \gtrsim c(t-t_0)$. However, at this point it is important to note that such displacement profile, which was derived assuming an infinite structure, is incompatible with a chain of finite length as that considered in Section 3, in which before initiation of the pulse all NN springs are in the undeformed configuration (i.e. for which $u_j = 0$). For such finite chain the displacement field takes the form (see Fig. 5(a))

$$u^{\text{finite}}(x,t) = \begin{cases} u(x,t), & 0 < x \le c_r(t-t_0); \\ 0, & c_r(t-t_0) < x \le (n-1)\,a, \end{cases} \tag{32}$$

where c_r is the velocity of the rarefaction front that is defined so that

$$u(c_r(t-t_0),t) = 0, \quad \text{with } c_r > c. \tag{33}$$

To determine $C_4(t)$ we impose momentum conservation, which, since the chain is initially at rest, reduces to

$$\partial_t \int_0^{(n-1)\,a} u^{\text{finite}}\mathrm{d}x = 0. \tag{34}$$

In Fig. 5(b) and (c) we report the temporal evolution of c_r and C_4 as found by numerically solving Eqs. (33) and (34) with u^{finite} given by Eq. (32). It is important to note that, in full agreement with our numerical results, our continuum model predicts a constant propagation velocity c_r for the rarefaction pulse. Next, to obtain explicit expressions for both c_r and C_4, we take advantage of the fact that the width of the transition region connecting the portions of the displacement profile

Please cite this article as: B. Deng, P. Wang and V. Tournat et al., Nonlinear transition waves in free-standing bistable chains, Journal of the Mechanics and Physics of Solids, https://doi.org/10.1016/j.jmps.2019.07.004

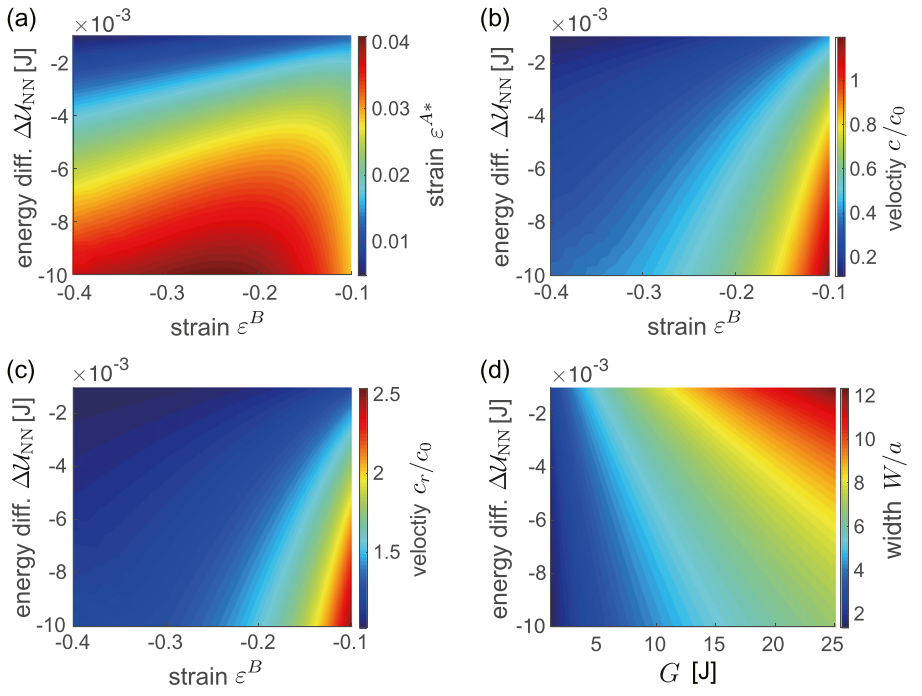

Fig. 6. (a) Evolution of ε^{A*} as a function of ε^B and $\Delta\mathcal{U}_{\rm NN}$ as predicted by Eq. (27). (b) Evolution of c/c_0 as a function of ε^B and $\Delta\mathcal{U}_{\rm NN}$ as predicted by Eq. (27). (c) Evolution of c_r/c_0 as a function of ε^B and $\Delta\mathcal{U}_{\rm NN}$ as predicted by Eq. (38). (d) Evolution of W/a as a function of G and $\Delta\mathcal{U}_{\rm NN}$ as predicted by Eq. (30).

with slope ε^B and ε^{A*} is narrow and approximate $u^{\rm finite}$ with a piece-wise linear function as

$$u^{\rm finite}(x,t) \approx \begin{cases} \varepsilon^B[x - c(t-t_0)] + C_4(t), & 0 < x \le c(t-t_0); \\ \varepsilon^{A*}[x - c(t-t_0)] + C_4(t), & c(t-t_0) < x \le c_r(t-t_0); \\ 0, & c_r(t-t_0) < x \le (n-1)\,a, \end{cases} \tag{35}$$

where (see Fig. 5(a))

$$C_4(t) \approx (c - c_r)\,(t - t_0)\,\varepsilon^{A*}. \tag{36}$$

Substitution of Eqs. (35) and (36) into Eq. (34) yields

$$\varepsilon^B\left[c + \frac{\varepsilon^{A*}}{\varepsilon^B}(c_r - c)\right]^2 + (c_r - c)^2\,\varepsilon^{A*}\left(1 - \frac{\varepsilon^{A*}}{\varepsilon^B}\right) = 0, \tag{37}$$

from which c_r is obtained as

$$c_r = c\sqrt{1 - \frac{\varepsilon^B}{\varepsilon^{A*}}}. \tag{38}$$

In Fig. 5(b) and (c) we also report the evolution of c_r and C_4 as predicted by Eqs. (38) and (36) and find excellent agreement with the numerical results, thus confirming the validity of our simplifications.

As a last step, the velocity along the chain can be obtained from Eqs. (31) and (36) as

$$v = \frac{\mathrm{d}u}{dt} = -\frac{(\varepsilon^{A*} - \varepsilon^B)c}{2}\,\tanh\left(\frac{x - c(t-t_0)}{W}\right) - \frac{(\varepsilon^{A*} + \varepsilon^B)c}{2} + (c - c_r)\varepsilon^{A*}, \tag{39}$$

from which the velocity of masses connected to NN springs deformed to ε^{A*} and ε^B can be obtained as,

$$\begin{aligned} v^{A*} &= v|_{x\to\infty} = -\varepsilon^{A*}\,c_r \\ v^B &= v|_{x\to-\infty} = -\varepsilon^B\,c + \varepsilon^{A*}(c - c_r), \end{aligned} \tag{40}$$

confirming that after transitioning to the lower-energy stable configuration all springs keep moving with constant velocity.

Please cite this article as: B. Deng, P. Wang and V. Tournat et al., Nonlinear transition waves in free-standing bistable chains, Journal of the Mechanics and Physics of Solids, https://doi.org/10.1016/j.jmps.2019.07.004

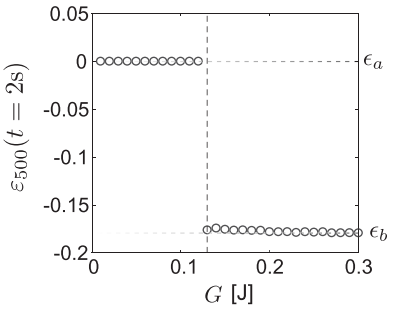

Fig. 7. Evolution of the strain for the 500th NN spring as a function of G at $t = 2$ s as predicted by our numerical simulations. We find that a transition wave propagates only if $G > 0.13$.

Comparison between analytical and numerical results

To test the validity of our continuum model, we compare the analytical predictions with the numerical results presented in Section 3. To begin with, we note that, in full agreement with our numerical results, our continuum model predicts that the considered chain supports a transition wave that propagates with constant velocity c and that is preceded by a rarefaction front with positive strain of ε^{A*} that also propagates with constant velocity, c_r. Notably, we also find an excellent quantitative agreement between analytical predictions and numerical results. Using the values introduced in Section 3, Eqs. (27) and (38) predict $c = 3.08$ m/s, $c_r = 11.41$ m/s and ε^{A*}=0.014, while according to our numerical simulations $c = 3.01$ m/s, $c_r = 11.35$ m/s and ε^{A*}=0.014 (see Fig. 2). Furthermore, in Fig. 2(d) we compare the strain and displacement distribution predicted by our model (via Eqs. (29) and (31)) and numerical simulations at $t = 1.2$ s. Again, we find that the analytical predictions (solid lines) match perfectly with the numerical results (markers) and capture the details of the transition zone between phase B and phase A^* (Fig. 2(e)). Finally, in Fig. 3 we report the analytically obtained velocity and strain for the three phases supported by the chain, (ε^A, v^A)=(0, 0), (ε^{A*}, v^{A*})=(0.014, -0.16 m/s) and (ε^B, v^B)=(−0.181, 0.44 m/s). Also in this case we find that the analytical model nicely captures the numerical results, confirming the validity of the assumptions made during its derivation.

Influence of system's parameters

Having confirmed the validity of our analytical model, we now use it to explore the effect of the system parameters on the propagation of the transition waves. First, we note that, according to Eqs. (27) and (38), ε^{A*}, c/c_0 and c_r/c_0 (c_0 being the velocity of linear vibrations in the long wavelength regime) only depend on the energy landscape of the NN springs $\mathcal{U}_{\mathrm{NN}}(\varepsilon)$, which is characterized by ε^B and $\Delta\mathcal{U}_{\mathrm{NN}}$. As shown in Fig. 6(a–c), we find that ε^{A*}, c and c_r all increase as the energy difference between the two stable configurations becomes larger and more energy is emitted by the NN springs during transition. Furthermore, c and c_r decreases as the stable strain ε^B becomes more negative, whereas ε^{A*} is not significantly affected by ε^B.

Second, our model predicts that the NNS interactions (quantified by G) only affect the width W of the transition zone (see Eq. (30)). In Fig. 6(d) we report the evolution of W/a as predicted by Eq. (30) as a function of G and $\Delta\mathcal{U}_{\mathrm{NN}}$. We find that larger G yield wider transition zones while larger energy differences result in sharper transition zones. Note that the dependency of W on G can also be investigated using Eq. (23), which describes the motion of a pseudo-particle of mass a^2G in the potential V_{pseudo}. More specifically, since the motion of the fictitious particle gets slower as its mass a^2G increases, Eq. (23) indicates that the transition zone becomes wider for structures characterized by a larger coupling constant G. This is consistent with the fact that the NNS interactions tend to homogenize the strain along the chain, creating smoother transition zones. Finally, we want to point out that, while according to the continuum model transition waves propagate through the chain for any G, our numerical simulations indicate that propagation is only possible if G is large enough to overcome the initial energy barrier. To investigate this point, we conduct additional numerical simulations using a chain with the same NN springs and initial condition considered in Section 3 and $G \in [0.01\,\mathrm{J}, 0.30\,\mathrm{J}]$. In Fig. 7 we report the strain of the 500-th NN spring, ε_{500}, at $t = 2$ s which is a sufficient long time for the transition wave (if triggered) to propagate through the entire chain. We find that for $G < 0.13$ J, $\varepsilon_{500} = \varepsilon^A = 0$ (indicating that the transition wave does not propagate through the system), whereas for $G > 0.13$ J the transition wave is triggered and $\varepsilon_{500} = \varepsilon^B$.

5. Conclusions

To summarize, we have used a combination of numerical and analytical tools to investigate the propagation of transition waves in a 1D array of masses connected by bistable springs and accounting for nearest neighboring spring (NNS) interactions. We have found that three well distinct phases emerge during propagation: (*i*) Phase A corresponding to the springs in their undeformed higher-energy stable configuration; (*ii*) Phase B corresponding to the springs in their deformed lower-energy stable configuration; and (*iii*) Phase A* - an intermediate stretched configuration that appears just before the

Please cite this article as: B. Deng, P. Wang and V. Tournat et al., Nonlinear transition waves in free-standing bistable chains, Journal of the Mechanics and Physics of Solids, https://doi.org/10.1016/j.jmps.2019.07.004

transition from Phase A to Phase B. Remarkably, we were also able to obtain closed-form analytical solutions that enables us to fully characterize each phase as well as the width and speed of the propagating waves.

While in this study we only considered 1D lattices, the proposed analytical tools can be further extended to capture the propagation of transition waves in 2D bistable systems (Rafsanjani and Pasini, 2016; Schaeffer and Ruzzene, 2015a; 2015b; 2015c). As such, we envision our model to provide opportunities to elucidate how transition waves propagate in both bistable mechanical metamaterials (Chen et al., 2019; Rafsanjani et al., 2016; Rafsanjani and Pasini, 2016; Schaeffer and Ruzzene, 2015a; 2015b; 2015c; Shan et al., 2015) and phase transforming materials (Nishiyama, 2012; Truskinovsky and Vainchtein, 2005) whose volume macroscopically changes as a result of the phase transition (Jones and Ashby, 2005).

Acknowledgements

KB acknowledges support from the National Science Foundation under Grant No. DMR-1420570 and EFMA-1741685 and from the Army Research Office under Grant No. W911NF-17-1-0147. VT acknowledges support from the program Acoustics Hub funded by a Connect Talent grant of the Region Pays de la Loire.

References

Aifantis, E.C., 1992. On the role of gradients in the localization of deformation and fracture. Int. J. Eng. Sci. 30, 1279–1299. doi:10.1016/0020-7225(92)90141-3.
Audoly, B., Hutchinson, J.W., 2016. Analysis of necking based on a one-dimensional model. J. Mech. Phys. Solids 97, 68–91.
Braun, O.M., Kivshar, Y.S., 1998. Nonlinear dynamics of the Frenkel–Kontorova model. Phys. Rep. 306 (1–2), 1–108.
Chen, T., Zhang, X., Yan, X., Zhang, B., Jiang, J., Huang, D., Qi, M., Sun, R., 2019. Harnessing magnets to design tunable architected bistable material. Adv. Eng. Mater. 1801255. doi:10.1002/adem.201801255.
Comte, J.-C., Marquié, P., Remoissenet, M., 1999. Dissipative lattice model with exact traveling discrete kink-soliton solutions: discrete breather generation and reaction diffusion regime. Phys. Rev. E 60 (6), 7484.
Dauxois, T., Peyrard, M., 2006. Physics of Solitons. Cambridge University Press.
Dye, D., 2015. Shape memory alloys: towards practical actuators. Nature Mater. 14 (8), 760.
Fiebig, M., Lottermoser, T., Meier, D., Trassin, M., 2016. The evolution of multiferroics. Nature Rev. Mater. 1 (8), 16046.
Frazier, M.J., Kochmann, D.M., 2017. Atomimetic mechanical structures with nonlinear topological domain evolution kinetics. Adv. Mater. 29 (19), 1605800.
Giri, P., Choudhary, K., Dey, A., Biswas, A., Ghosal, A., Bandyopadhyay, A., 2012. Discrete energy levels of bright solitons in lithium niobate ferroelectrics. Phys. Rev. B 86 (18), 184101.
Jones, D.R., Ashby, M.F., 2005. Engineering Materials 2: An Introduction to Microstructures, Processing and Design. Elsevier.
Katz, S., Givli, S., 2018. Solitary waves in a bistable lattice. Extreme Mech. Lett. 22, 106–111. doi:10.1016/j.eml.2018.06.003.
Nadkarni, N., Arrieta, A.F., Chong, C., Kochmann, D.M., Daraio, C., 2016a. Unidirectional transition waves in bistable lattices. Phys. Rev. Lett. 116 (24), 244501.
Nadkarni, N., Daraio, C., Abeyaratne, R., Kochmann, D.M., 2016b. Universal energy transport law for dissipative and diffusive phase transitions. Phys. Rev. B 93 (10), 104109.
Nadkarni, N., Daraio, C., Kochmann, D.M., 2014. Dynamics of periodic mechanical structures containing bistable elastic elements: from elastic to solitary wave propagation. Phys. Rev. E 90 (2), 023204.
Nishiyama, Z., 2012. Martensitic Transformation. Elsevier.
Polyanin, A., Zaitsev, V., 2011. Handbook of Nonlinear Partial Differential Equations, Second Edition. Chapman and Hall/CRC.
Rafsanjani, A., Akbarzadeh, A, Pasini, D., 2015. Snapping mechanical metamaterials under tension. dvanced Materials 27 (39), 5931–5935.
Rafsanjani, A., Jin, L., Deng, B., Bertoldi, K., 2019. Propagation of pop ups in kirigami shells. Proc. Natl. Acad. Sci. 2018–17763.
Rafsanjani, A., Pasini, D., 2016. Bistable auxetic mechanical metamaterials inspired by ancient geometric motifs. Extreme Mech. Lett. 9, 291–296.
Raney, J.R., Nadkarni, N., Daraio, C., Kochmann, D.M., Lewis, J.A., Bertoldi, K., 2016. Stable propagation of mechanical signals in soft media using stored elastic energy. Proc. Natl. Acad. Sci. doi:10.1073/pnas.1604838113.
Remoissenet, M., Peyrard, M., 1984. Soliton dynamics in new models with parametrized periodic double-well and asymmetric substrate potentials. Phys. Rev. B 29 (6), 3153.
Schaeffer, M., Ruzzene, M., 2015a. Comptes rendus mecanique dynamic reconfiguration of magneto-elastic lattices. Comptes Rendus Mecan. 343 (12), 670–679. doi:10.1016/j.crme.2015.06.007.
Schaeffer, M., Ruzzene, M., 2015b. Homogenization of 1D and 2D magnetoelastic lattices. EPJ Appl. Metamater. 2, 13. doi:10.1051/epjam/2015013.
Schaeffer, M., Ruzzene, M., 2015c. International journal of solids and structures wave propagation in multistable magneto-elastic lattices. Int. J. Solids Struct. 56–57, 78–95. doi:10.1016/j.ijsolstr.2014.12.003.
Shan, S., Kang, S.H., Raney, J.R., Wang, P., Fang, L., Candido, F., Lewis, J.A., Bertoldi, K., 2015. Multistable architected materials for trapping elastic strain energy. Adv. Mater. 27 (29), 4296–4301.
Slepyan, L., 2000. Dynamic factor in impact, phase transition and fracture. J. Mech. Phys. Solids 48 (5), 927–960.
Slepyan, L., 2001. Feeding and dissipative waves in fracture and phase transition: II. phase-transition waves. J. Mech. Phys. Solids 49 (3), 513–550.
Slepyan, L., Cherkaev, A., Cherkaev, E., 2005. Transition waves in bistable structures. ii. analytical solution: wave speed and energy dissipation. J. Mech. Phys. Solids 53 (2), 407–436.
Truskinovsky, L., Vainchtein, A., 2005. Kinetics of martensitic phase transitions: lattice model. SIAM J. Appl. Math. 66 (2), 533–553.
Wazwaz, A.-M., 2007. New solitons and kink solutions for the gardner equation 12 (8), 1395–1404. Exported from on 2018/10/17 doi: 10.1016/j.cnsns.2005.11.007.
Wojnar, C., le Graverend, J.-B., Kochmann, D., 2014. Broadband control of the viscoelasticity of ferroelectrics via domain switching. Appl. Phys. Lett. 105 (16), 162912.

Please cite this article as: B. Deng, P. Wang and V. Tournat et al., Nonlinear transition waves in free-standing bistable chains, Journal of the Mechanics and Physics of Solids, https://doi.org/10.1016/j.jmps.2019.07.004